A robust type-2 fuzzy sliding mode controller for disturbed MIMO nonlinear systems with unknown dynamics

Nabil Nafia, Abdeljalil El Kari, Hassan Ayad & Mostafa Mjahed

Published online: 19 Sep 2018.

Submit your article to this journal ⬀

Article views: 298

View related articles ⬀

View Crossmark data ⬀

Taylor & Francis
Taylor & Francis Group

REGULAR PAPER

🔓 OPEN ACCESS   ⟳ Check for updates

A robust type-2 fuzzy sliding mode controller for disturbed MIMO nonlinear systems with unknown dynamics

Nabil Nafia[a], Abdeljalil El Kari[a], Hassan Ayad[a] and Mostafa Mjahed [b]

[a]Laboratory of Electric System and Telecommunication (LSET), Faculty of Sciences and Techniques Guéliz (FSTG), University Cadi Ayyad, Marrakech, Morocco; [b]Royal School of Aeronautic (ERA), Marrakech, Morocco

ABSTRACT

In this paper, in order to achieve the best tracking control of a class of multi-input multi-output (MIMO) nonlinear systems with unknown dynamics and unknown disturbances, a new robust adaptive interval type-2 fuzzy sliding mode control law (AIT2-FSMCL) has been proposed. Based on developing interval type-2 fuzzy local models for some operating points of the controlled system, an interval type-2 fuzzy logic system (IT2-FLS) has been designed to better estimate the unknown nonlinear dynamics of the studied system. Then, to enhance the tracking control performance and ensure the system robustness in the presence of approximation errors, parameter variations, un-modelled dynamics and external disturbances, a new AIT2-fuzzy sliding mode system (AIT2-FSMS), has been introduced. In order to avoid the chattering phenomenon while keeping the system performance, the AIT2-FSMS uses three AIT2-fuzzy logic systems (AIT2-FLSs) to estimate the optimal gains of the AIT2-FSMCL. The adaptation laws have been derived using the Lyapunov stability approach. The mathematical proof shows that the closed-loop system with the proposed control approach is globally asymptotically stable. Finally, the proposed design method is applied to a two-link robot arm to validate the effectiveness of the proposed control approach.

1. Introduction

Conventionally, control algorithms can hardly deal with multi-input multi-output (MIMO) uncertain nonlinear systems. To cope with this problem of control, several robust approaches have been proposed. Among them, fuzzy logic control (FLC), H_∞ technique and sliding mode control (SMC) have attracted a remarkable attention.

Over the past decades, intelligent algorithms using fuzzy logic systems (FLSs) have been extensively used and successfully applied in various applications [1–9]. However, for nonlinear perturbed complex systems with uncertainties, FLSs cannot guarantee the global stability of the closed-loop system [10]. To overcome this problem, many researchers have tried to combine FLSs with other advanced robust methods to achieve good performance, such as SMC, adaptive control, H_∞ technique and neural network [11–16]. In [17], the authors have proposed an adaptive sliding mode controller for systems with actuator saturation to guarantee that the closed-loop system is uniformly ultimately bounded. In [18], an adaptive fuzzy SMC (AFSMC) for uncertain discrete-time nonlinear systems is proposed. The nonlinear uncertainties are approximated by using a fuzzy system. Then, an AFSMC term is added to the control to compensate the modelling errors. And,

in [19], a discrete sliding mode controller for a class of nonlinear systems described by a Takagi-Sugeno (T-S) fuzzy model subject to modelling error has been proposed to guarantee the global stability of the closed-loop system despite the modelling error.

SMC is a particular kind of robust control, which allows the complete reject of any disturbances acting on the system dynamics. It has been successfully applied for many complex uncertain perturbed systems [20–24]. However, the control law in the conventional SMC is discontinuous, which can generate the so-called chattering phenomenon [25,26]. This phenomenon consists of the oscillation of the control law at a frequency and with amplitude capable of damaging the actuators [26]. In order to reduce the chattering, boundary layer methods (BL) and higher order SMC approaches (HO-SMC) are usually adopted by many researchers [27–30]. However, these methods have a major disadvantage that limits their performance which consists in the fact that they require the knowledge of the upper bounds of the different kinds of uncertainties and disturbances that affect the system dynamics. Moreover, the HO-SMC algorithms require in general higher order derivative of the sliding variable. And, the BL approach constraint the system state trajectories not to the desired dynamics but to their vicinities,

---

thus losing the control accuracy and may even provoke a deterioration of the system stability. The second-order super-twisting SMC (SOST-SMC) is among the most popular and effective HO-SMC algorithms widely used in the literature for controlling complex uncertain non-linear systems [31–36], it is developed by Levant [37] to avoid the chattering and ensure the finite time convergence of the system state trajectories. However, the choice of its control gains values remains one of the major problems for this kind of algorithms. The large gains can cause the chattering and a dynamic response with overshoot. And, the small gains can deteriorate the tracking control accuracy and affect the system robustness.

On the other hand, FLS cannot directly handle rule and measurement uncertainties because it uses type-1 fuzzy sets (T1-FSs) that are certain. To cope with this constraint, the so-called type-2 fuzzy logic system (T2-FLS) has been introduced in designing robust controllers and becomes more and more imposed in industrial and technological fields [38–40]. One reason is that a T2-FS is characterized by a membership function (MF) that includes a footprint of uncertainty (FOU) which makes it possible to handle linguistic uncertainties more effectively than T1-FLSs [41,42]. In [43], both the position and speed of a mobile robot are controlled by using two interval type-2 fuzzy controllers. And, in [44], both the position and speed of a mobile robot are controlled by using two interval type-2 fuzzy controllers.

Compared to the existing works in the literature, the main contributions of the present study are listed as follows:

(1) A new robust adaptive interval type-2 fuzzy sliding mode control law (AIT2-FSMCL) is proposed for a large class of MIMO nonlinear systems to deal with the tracking control problem, with the following considerations are taken into account:
   • All dynamics are entirely unknown and suffer from time varying disturbances.
   • No prior knowledge is required for the upper bound of unknown disturbances that affect the studied system dynamics, including un-modelled dynamics such as friction force, parametric variations and external disturbances.
(2) Based on T-S fuzzy system characterized by its ability to represent input/output relationships locally of a system [45], an interval T2-FLS (IT2-FLS), has been introduced in order to efficiently describe the unknown dynamics of the studied system. FSs are chosen to be IT2, firstly, because they do not require a lot of computation and, secondly, for their efficiency to capture severe uncertainties.
(3) A new synthesized AIT2-fuzzy sliding mode system (AIT2-FSMS) has been introduced to handle modelling errors and effectively reject the effects

of parametric variations, un-modelled dynamics and unknown external disturbances on the system dynamics. By using three AIT2-FLSs, the AIT2-FSMS is designed in such a way as to generate the optimal gains of the AIT2-FSMCL that ensure the best tracking control performance while simultaneously avoiding the undesired chattering.
(4) The adaptation laws are derived using the Lyapunov stability theorem. Finally, a two-link robot arm is used as a study case to confirm the effectiveness of the proposed control approach.

This paper is organized as follows. Section 2 describes the IT2-FLSs. In Section 3, the problem formulation is presented. In Section 4, we propose the controller design method. Finally, the simulation results are illustrated in Section 5.

2. Introduction to type-2 fuzzy logic systems

A T2-FLS is characterized by MFs that are themselves fuzzy. Output sets of inference engine are T2-FSs. Therefore, a reducer is required to convert them into T1-FS. The obtained type reducer set is then defuzzified to obtain a crisp output.

An example of a T2 fuzzy MF is the Gaussian MF represented in Figure 1, with the associated FOU, is the area in between the upper and lower MFs.

Upper MF and lower MF are two T1 fuzzy MFs. $\mu 1$ is the intersection of the crisp input x with lower MF, and $\mu 2$ is the intersection with upper MF.

2.1. Interval type-2 fuzzy modelling system

The T-S fuzzy system is characterized by its ability to represent input/output relationships locally of a system. Every conclusion of such system is expressed by a linear system describing the system dynamics at a given operating point. Then, with a rule base of M rules, each having q antecedents and p consequents, the jth rule can be written as [45]

$$R^j : \text{if } x_1 \text{ is } F_1^j \text{ and } x_2 \text{ is } F_2^j \ldots \text{ and } x_q \text{ is } F_q^j$$

$$\text{then } \begin{cases} x^{(n)} = A_j \underline{x} + B_j u \\ y = x \end{cases} \tag{1}$$

where F_i^j are the antecedent FSs characterized by the fuzzy MFs $\mu_{F_i^j}(x_i)$; $x = [\,x_1 \; x_2 \; \ldots \; x_p\,]^{\mathrm{T}}$ is the first element of the state vector $\underline{x} = [x^T, \dot{x}^T, \ldots, x^{(n-1)T}]^{\mathrm{T}} \in \mathbb{R}^q$ such that $q = p \times n$; $u \in \mathbb{R}^m$ and $y \in \mathbb{R}^p$ are, respectively, the input and the output of the studied system; $A_j \in \mathbb{R}^{p \times q}$ is the state matrix and $B_j \in \mathbb{R}^{p \times m}$ denotes the input matrix.

In this study, to take advantage of the potential of T2-FS to consider uncertainties on T2 fuzzy rules, FSs F_i^j defined in (1) are replaced by IT2-FSs. Then, the system (1) can be reformulated using the T-S rule based
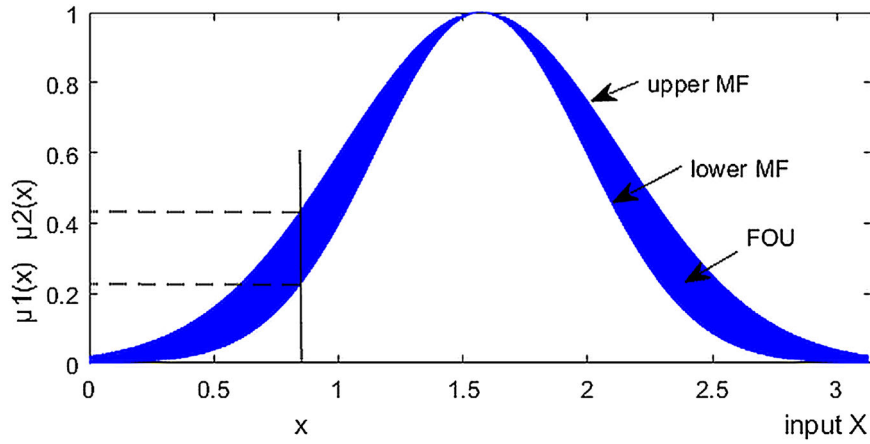
Figure 1. A type-2 fuzzy set.

modelling for a T2 fuzzy system as follows:

$$R^j : \text{ if } x_1 \text{ is } \tilde{F}_1^j \text{ and } x_2 \text{ is } \tilde{F}_2^j \dots \text{ and } x_q \text{ is } \tilde{F}_q^j$$

$$\text{then } \begin{cases} x^{(n)} = A_j \underline{x} + B_j u \\ y = x \end{cases} \quad (2)$$

where $\tilde{F}_i^j$ are IT2-FSs characterized by the fuzzy MFs $\mu_{\tilde{F}_i^j}(x_i)$

Consider that all local models of the system (2) are controllable and the meet operation is implemented by the product t-norm. Then, the firing interval of the jth fuzzy rule is the following interval T1-FS (IT1-FS):

$$Z^j(\underline{x}) = [z_l^j(\underline{x}), z_r^j(\underline{x})] \quad (3)$$

where $z_l^j(\underline{x}) = \prod_{i=1}^{q} \mu_{\tilde{F}_i^j}^{\text{low}}(x_i)$ and $z_r^j(\underline{x}) = \prod_{i=1}^{q} \mu_{\tilde{F}_i^j}^{\text{upp}}(x_i)$, with $\mu_{\tilde{F}_i^j}^{\text{low}}(x_i)$ and $\mu_{\tilde{F}_i^j}^{\text{upp}}(x_i)$ are the lower and upper MFs of $\mu_{\tilde{F}_i^j}(x_i)$, respectively.

2.2. Type reduction for interval type-2 fuzzy sets

The output of the inference engine must be reduced to a T1-FS before defuzzification. The type reduction using the centre of sets (COS) method is adopted in this study for the IT2-FSs and it is given by [46]

$$Y_{\cos}(\theta^1, \theta^2, \dots, \theta^M, Z^1, Z^2, \dots, Z^M)$$

$$= \int_{y^1} \int_{y^2} \cdots \int_{y^M} \int_{z^1} \int_{z^2} \cdots$$

$$\int_{z^M} \frac{1 / \sum_{j=1}^{M} y^j z^j (dy^1 dy^2 \dots dy^M dz^1 dz^2 \dots dz^M)}{\sum_{j=1}^{M} z^j}$$

$$\quad (4)$$

where $Y_{\cos}$ is an IT1-FS defined by two end points $y_l(\underline{x})$ and $y_r(\underline{x})$; $y^j \in \theta^j = [\theta_l^j, \theta_r^j]$ with θ^j is the centroid of the associated fuzzy consequent set; and $z^j \in Z^j(\underline{x}) = [z_l^j(\underline{x}), z_r^j(\underline{x})]$.

The defuzzified crisp output by using the centre of gravity is then obtained as follows:

$$y = \frac{y_l + y_r}{2} \quad (5)$$

where y_l and y_r can be expressed as

$$\begin{cases} y_l = \min_{Z^j} \frac{\sum_{j=1}^{M} \theta_l^j z^j}{\sum_{j=1}^{M} z^j} = \theta_l^T \xi_l \\ \\ y_r = \max_{Z^j} \frac{\sum_{j=1}^{M} \theta_r^j z^j}{\sum_{j=1}^{M} z^j} = \theta_r^T \xi_r \end{cases} \quad (6)$$

where $\xi_l = [\xi_l^1 \, \xi_l^2 \, \dots \, \xi_l^M]^T$ and $\xi_r = [\xi_r^1 \, \xi_r^2 \, \dots \, \xi_r^M]^T$ are two vectors of fuzzy basis functions, such that: $\xi_l^j = \frac{z^j}{\sum_{j=1}^{M} z^j}$ and $\xi_r^j = \frac{\bar{z}^j}{\sum_{j=1}^{M} \bar{z}^j}$, with $(\underline{z}^j, \bar{z}^j) \in Z^j(\underline{x})$; $\theta_l = [\theta_l^1 \, \theta_l^2 \, \dots \, \theta_l^M]^T$ and $\theta_r = [\theta_r^1 \, \theta_r^2 \, \dots \, \theta_r^M]^T$ are the adjustable parameter vectors.

In this study, $\underline{z}^j$ and $\bar{z}^j$ are determined using the iterative algorithm developed by Mendel and Karnik [47]. Therefore, y_l and y_r can be easily computed.

3. Problem formulation

Consider a general class of MIMO nth order nonlinear systems, having m inputs and p outputs ($p \leq m$), described by the following equation:

$$\begin{cases} x^{(n)} = f(\underline{x}) + g(\underline{x})u + d \\ y = x \end{cases} \quad (7)$$

where $f(\underline{x}) = f_N(\underline{x}) + \Delta f(\underline{x}) = [f_1 \, f_2 \, \dots \, f_p] \in \mathbb{R}^p$ is a vector of bounded unknown nonlinear continuous functions, and $g(\underline{x}) = g_N(\underline{x}) + \Delta g(\underline{x}) =$

$$\begin{bmatrix} g_{1,1} & g_{1,2} & \cdots & g_{1,m} \\ g_{2,1} & g_{2,2} & \cdots & g_{2,m} \\ \vdots & \vdots & \vdots & \vdots \\ g_{p,1} & g_{p,2} & \cdots & g_{p,m} \end{bmatrix} \in \mathbb{R}^{p \times m}$$ is a matrix of bounded

unknown nonlinear continuous functions, with $\Delta f(\underline{x})$ and $\Delta g(\underline{x})$ represent the parametric variation on the system dynamics; $u = [u_1 \, u_2 \, \dots \, u_m]^T \in \mathbb{R}^m$ and $y \in \mathbb{R}^p$,

are, respectively, the input and the output of the system; $\underline{x} = [x^T, \dot{x}^T, \ldots, x^{(n-1)T}]^T \in \mathbb{R}^q$ denotes the state vector of the system assumed to be available to measurement, with $x = [\,x_1\ x_2\ \ldots\ x_p\,]^T$ is the first element of the state vector, and $q = n \times p$; $d = [\,d_1\ d_2\ \ldots\ d_p\,] \in \mathbb{R}^p$ denotes unknown bounded disturbances, including un-modelled and unknown external disturbances.

Assume that $g_N(\underline{x})$ is a non-null matrix, and let $g_N^{-1}(\underline{x})$ denote the Moore-Penrose pseudo-inverse of $g_N(\underline{x})$.

Based on the system (2), for a given state/control $(\underline{x}, u)$ pair of the system (7), if the product is used as an inference engine, COS for the type reduction and the centre of gravity for defuzzification. The defuzzified crisp out will appear as a weighted average of the IT2 fuzzy local models:

$$\begin{cases} x^{(n)} = \dfrac{\sum_{j=1}^{M} z^j(\underline{x})[A_j\underline{x} + B_ju]}{\sum_{j=1}^{M} z^j(\underline{x})} \\[4mm] \quad = \dfrac{1}{2}\dfrac{\sum_{j=1}^{M} \underline{z}^j(\underline{x})[A_j\underline{x} + B_ju]}{\sum_{j=1}^{M} \underline{z}^j(\underline{x})} \\[4mm] \quad + \dfrac{1}{2}\dfrac{\sum_{j=1}^{M} \bar{z}^j(\underline{x})[A_j\underline{x} + B_ju]}{\sum_{j=1}^{M} \bar{z}^j(\underline{x})} \\[4mm] y = x \end{cases} \tag{8}$$

Let $f_0(\underline{x}) = [\,f_0^1\ f_0^2\ \ldots\ f_0^p\,]^T = \dfrac{1}{2}\left[\dfrac{\sum_{j=1}^{M} \underline{z}^j A_j \underline{x}}{\sum_{j=1}^{M} \underline{z}^j} + \dfrac{\sum_{j=1}^{M} \bar{z}^j A_j \underline{x}}{\sum_{j=1}^{M} \bar{z}^j}\right]$

and $g_0(\underline{x}) = \begin{bmatrix} g_{1,1}^0 & g_{1,2}^0 & \cdots & g_{1,m}^0 \\ g_{2,1}^0 & g_{2,2}^0 & \cdots & g_{2,m}^0 \\ \vdots & \vdots & \vdots & \vdots \\ g_{p,1}^0 & g_{p,2}^0 & \cdots & g_{p,m}^0 \end{bmatrix}$

$= \dfrac{1}{2}\left[\dfrac{\sum_{j=1}^{M} \underline{z}^j B_j}{\sum_{j=1}^{M} \underline{z}^j} + \dfrac{\sum_{j=1}^{M} \bar{z}^j B_j}{\sum_{j=1}^{M} \bar{z}^j}\right]$; then, the system (8) can be reformulated as

$$\begin{cases} x^{(n)} = f_0(\underline{x}) + g_0(\underline{x})u \\ y = x \end{cases} \tag{9}$$

The system (9) is an IT2-FLS designed to describe the unknown dynamics of the system (7).

Consider $\varepsilon_f(\underline{x})$ and $\varepsilon_g(\underline{x})$ the approximation errors of $f_N(\underline{x})$ and $g_N(\underline{x})$, respectively. Thus, $f_N(\underline{x})$ and $g_N(\underline{x})$ can be formulated respectively as follows:

$$\begin{cases} f_N(\underline{x}) = f_0(\underline{x}) + \varepsilon_f(\underline{x}) \\ g_N(\underline{x}) = g_0(\underline{x}) + \varepsilon_g(\underline{x}) \end{cases} \tag{10}$$

Then, the system (7) can be rewritten as

$$\begin{cases} x^{(n)} = f_0(\underline{x}) + g_0(\underline{x})u + \varphi \\ y = x \end{cases} \tag{11}$$

where $\varphi = [\,\varphi_1\ \varphi_2\ \ldots\ \varphi_p\,]^T = (\Delta f(\underline{x}) + \varepsilon_f(\underline{x})) + (\Delta g(\underline{x}) + \varepsilon_g(\underline{x}))u + d$ is assumed to be bounded $((|\varphi_i| \leq \phi_i, \phi_i \geq 0,\ i = 1, \ldots, p)$.

4. Control law design

The control objective is to ensure that the state x tracks the desired reference $x_r = [\,x_r^1\ x_r^2\ \ldots\ x_r^p\,]^T$ in the presence of un-modelled dynamics, parametric variations and unknown external disturbances for a large class of MIMO nonlinear systems with unknown dynamics as it was defined in (7). Therefore, in order to guarantee the robustness of the system (7) against these constraints and ensure the best tracking control performance while simultaneously avoiding the undesired chattering, a new AIT2-FSMCL is proposed in this study.

4.1. Sliding mode control law design

The main objective of SMC is to force the system dynamics to reach and then remain on the sliding surface $s(\underline{x}, t) = \underline{0}$, with $\underline{0} \in \mathbb{R}^p$ denotes the null vector.

Define the tracking error $e = x_r - x$. Then, the sliding surface can be defined for a nth order system as [48]

$$\begin{aligned} s(\underline{x}, t) &= \begin{bmatrix} s_1 & s_2 & \ldots & s_p \end{bmatrix}^T \in \mathbb{R}^p \\[2mm] &= \left(\dfrac{\partial}{\partial t} + \lambda\right)^{(n-1)} e \\[2mm] &= \sum_{j=0}^{n-1} \dfrac{(n-1)!}{j!(n-j-1)!}\left(\dfrac{\partial}{\partial t}\right)^{(n-j-1)} \lambda^j e \end{aligned} \tag{12}$$

where $\lambda = \text{diag}(\lambda_i)_{1 \leq i \leq p} \in \mathbb{R}^{(p \times p)}$, is a diagonal matrix, with λ_i is the positive slope of the sliding surface s_i.

In order to ensure the desired control performance, a new control law is designed as follows:

$$\begin{aligned} u &= g_0^{-1}(\underline{x})(x_r^{(n)} - f_0(\underline{x}) + \rho - u_c) \\ &= u_{eq} - g_0^{-1}u_c \end{aligned} \tag{13}$$

where $u_{eq} = g_0^{-1}(x_r^{(n)} - f_0(\underline{x}) + \rho)$ and u_c is a reaching sliding mode control law.

The fuzzy equivalent control u_{eq} describes the sliding mode of the system dynamics, it drives the system trajectories to the desired dynamics, and it is obtained when $\dot{s} = \underline{0}$. However, the approximation errors and unknown disturbances that affect the system (7) may cause a deterioration of the sliding mode. Therefore, a new robust reaching sliding mode control law u_c is introduced to overcome this problem. The control law u_c describes the reaching phase of the system state trajectories towards the sliding surface $s = \underline{0}$. Thus, the proposed reaching sliding mode control law is designed as follows:

$$\begin{aligned} u_c &= \begin{bmatrix} u_c(1) & u_c(2) & \ldots & u_c(p) \end{bmatrix}^T \\[2mm] &= -\alpha s(\underline{x}, t) - k\int_0^{t^r} sign(s(\underline{x}, t))\mathrm{d}t - \mu\omega(s(\underline{x}, t)) \end{aligned} \tag{14}$$

where $\omega(s(\underline{x},t)) = [\,\omega_1(s_1)\ \omega_2(s_2)\ ...\ \omega_p(s_p)\,]^T \in \mathbb{R}^p$, such that $\omega_i(s_i) = \begin{cases} \varepsilon_i\,\mathrm{sign}(s_i), s_i \in \Omega \\ \dfrac{\mathrm{sign}(s_i)}{\log^2|s_i|}, s_i \notin \Omega \end{cases}, \Omega = \{s_i \in s||s_i| \geq \frac{N_i}{2},$

$0 < N_i \leq 1\}$, and $\varepsilon_i = \frac{1}{\log^2(N_i/2)}$ in order to ensure a continuous signal in $|s_i| = (N_i/2)$; $\alpha = \mathrm{diag}(\alpha_i)_{1 \leq i \leq p}$, $\mu = \mathrm{diag}(\mu_i)_{1 \leq i \leq p}$ and $k = \mathrm{diag}(k_i)_{1 \leq i \leq p}$ are diagonal matrices of the positive reaching control gains α_i, μ_i and k_i, respectively; $\int_0^{t^r} \mathrm{sign}(s)dt = [\, \int_0^{t_1^r} \mathrm{sign}(s_1)dt$ $\int_0^{t_2^r} \mathrm{sign}(s_2)dt \ldots \int_0^{t_p^r} \mathrm{sign}(s_p)dt\,]^T$, with $t^r = [\, t_1^r\ t_2^r\ ...\ t_p^r\,]^T$ such that $t_i^r = \begin{cases} t & |s_i| > \vartheta_i \\ t_{\vartheta_i} & |s_i| \leq \vartheta_i \end{cases}$ denotes the reaching time to a neighborhood ϑ_i of the sliding surface $s_i = 0$.

Theorem 1: *For the controlled MIMO nonlinear system (7), with the IT2-FLS defined in (9), the control law defined in (13) is globally stable in closed-loop system with the tracking error converges asymptotically to zero, despite unknown dynamics and unknown disturbances that affect the system (7), including un-modelled dynamics, parametric variations and unknown external disturbances.*

Proof: In order to ensure the desired dynamics and guarantee the stability of the closed-loop control system, we consider the following Lyapunov function:

$$v = \frac{1}{2}s^T s \qquad (15)$$

The time derivative of the above equation for the system (11) can be given as

$$\dot{v} = s^T \dot{s}(\underline{x},t)$$
$$= s^T(x_r^{(n)} - f_0(\underline{x}) - g_0(\underline{x})u - \varphi + \rho) \qquad (16)$$

where $\rho = [\, \rho_1\ \rho_2\ ...\ \rho_p\,]^T = \sum_{j=1}^{n-1} \frac{(n-1)!}{j!(n-j-1)!} \left(\frac{\partial}{\partial t}\right)^{(n-j-1)} \lambda^j \dot{e}$

From (13), we get:

$$x_r^{(n)} = f_0(\underline{x}) + g_0(\underline{x})u + u_c - \rho \qquad (17)$$

Substitute $x_r^{(n)}$ and u_c by their expressions defined in (17) and (14), respectively, into (16), gives

$$\dot{v} = -\left(s^T\alpha s(\underline{x},t) \right.$$
$$\left. +s^T k \int_0^{t^r} \mathrm{sign}(s(\underline{x},t))\,\mathrm{d}t + s^T\mu\omega(s(\underline{x},t)) \right) - s^T\varphi \qquad (18)$$

The above equation becomes negative if the inequality below is guaranteed:

$$\alpha_i|s_i| + k_i t_i^r + \mu_i|\omega_i| \geq \phi_i, \quad i = 1,\ldots,p \qquad (19)$$

Thus, a good choice of the reaching control gains μ_i, α_i and k_i will allow verifying the above inequality (19),

hence, the proof 1 is completed. However, in practice, it is very difficult to obtain the optimal reaching control gains μ_i, α_i and k_i that ensure the best tracking control without deteriorating the system robustness. The large gains generate a big chattering in the system control and a dynamic response with overshoot, and the small ones affect the tracking accuracy and can even cause the instability in control system. In this paper, for handling this problem, a new AIT2-FSMS is designed to better estimate the optimal gains of μ_i, α_i and k_i that provide the best tracking control performance for the system (7) by guaranteeing the condition (19) and to simultaneously avoid the chattering phenomenon. ∎

4.2. Adaptive interval type-2 fuzzy sliding mode control law

Based on the IT2-FLS (5), and with the sliding surface $s(\underline{x},t)$ as an input vector, the terms $-\alpha s(\underline{x},t)$, $-k\int_0^{t^r} \mathrm{sign}(s)\,\mathrm{d}t$ and $-\mu\omega(s)$ of the control law defined in (14) are substituted by their AIT2-FLSs, respectively:

$$\hat{u}_\alpha(i) = \xi_\alpha^T(i)\theta_\alpha(i)|s_i|$$
$$\hat{u}_k(i) = \xi_k^T(i)\theta_k(i)t_i^r \qquad i = 1,\ldots,p \qquad (20)$$
$$\hat{u}_\mu(i) = \xi_\mu^T(i)\theta_\mu(i)|\omega_i(s_i)|$$

where $\xi_\alpha(i) = \frac{1}{2}(\xi_\alpha(i)_l + \xi_\alpha(i)_r) = [\,\xi_\alpha^1(i)\ \xi_\alpha^2(i)\ ...\ \xi_\alpha^M(i)\,]^T$, $\xi_k(i) = \frac{1}{2}(\xi_k(i)_l + \xi_k(i)_r) = [\,\xi_k^1(i)\ \xi_k^2(i)\ ...\ \xi_k^M(i)\,]^T$ and $\xi_\mu(i) = \frac{1}{2}(\xi_\mu(i)_l + \xi_\mu(i)_r) = [\,\xi_\mu^1(i)\ \xi_\mu^2(i)\ ...\ \xi_\mu^M(i)\,]^T$ are the vectors of fuzzy basis functions as they were described in (6); $\theta_\alpha(i) = [\,\theta_\alpha^1(i)\ \theta_\alpha^2(i)\ ...\ \theta_\alpha^M(i)\,]^T$, $\theta_k(i) = [\,\theta_k^1(i)\ \theta_k^2(i)\ ...\ \theta_k^M(i)\,]^T$ and $\theta_\mu(i) = [\,\theta_\mu^1(i)\ \theta_\mu^2(i)\ ...\ \theta_\mu^M(i)\,]^T$ are parameter vectors free to be designed by adaptive laws; M is the number of rules.

Define the optimal parameters of the AIT2-FLSs $\hat{u}_\alpha(i)$, $\hat{u}_k(i)$ and $\hat{u}_\mu(i)$:

$$\theta_\alpha^*(i) = \arg\min_{\theta_\alpha(i)}(\sup_{s_i}|\hat{u}_\alpha(i) - u_\alpha(i)|)$$

$$\theta_k^*(i) = \arg\min_{\theta_k(i)}(\sup_{s_i}|\hat{u}_k(i) - u_k(i)|) \qquad (21)$$

$$\theta_\mu^*(i) = \arg\min_{\theta_\mu(i)}(\sup_{s_i}|\hat{u}_\mu(i) - u_\mu(i)|)$$

The global proposed AIT2-FSMCL is designed as follows:

$$u = g_0^{-1}(\underline{x})(x_r^{(n)} - f_0(\underline{x}) + \rho - \hat{u}_c) \qquad (22)$$

where $\hat{u}_c = [\, \hat{u}_c(1)\ \hat{u}_c(2)\ ...\ \hat{u}_c(p)\,]^T = \hat{u}_\alpha + \hat{u}_k + \hat{u}_\mu$, such that: $\hat{u}_\alpha = [\, \hat{u}_\alpha(1)\ \hat{u}_\alpha(2)\ ...\ \hat{u}_\alpha(p)\,]^T$, $\hat{u}_k = [\, \hat{u}_k(1)\ \hat{u}_k(2)\ ...\ \hat{u}_k(p)\,]^T$ and $\hat{u}_\mu = [\, \hat{u}_\mu(1)\ \hat{u}_\mu(2)\ ...\ \hat{u}_\mu(p)\,]^T$.

The adaptive laws for the designed AIT2-FLSs defined in (20) are designed as follows:

$$\dot{\theta}_\alpha(i) = -\gamma_\alpha(i)s_i^2\text{sign}(s_i)\xi_\alpha(i)$$

$$\dot{\theta}_k(i) = -\gamma_k(i)s_i t_i^r \xi_k(i) \qquad (23)$$

$$\dot{\theta}_\mu(i) = -\gamma_\mu(i)s_i|\omega_i(s_i)|\xi_\mu(i)$$

where $\gamma_\alpha(i)$, $\gamma_k(i)$ and $\gamma_\mu(i)$ are positive constants

Theorem 2: *For the MIMO nonlinear system (7), with the IT2-FLS defined in (9), the AIT2-FLSs proposed in (20) and the adaptive laws expressed by Equation (23), the designed AIT2-FSMCL (22) is smooth and globally stable in closed-loop system with the tracking error converges asymptotically to zero, despite unknown dynamics and unknown disturbances that affect the system (7), including un-modeled dynamics, parametric variations and unknown external disturbances.*

Proof: Consider the following new augmented Lyapunov function:

$$v = \sum_{i=1}^{p} v_i = \frac{1}{2}\sum_{i=1}^{p} s_i^2 + \frac{1}{2}\sum_{i=1}^{p}\frac{\tilde{\theta}_\alpha^T(i)\tilde{\theta}_\alpha(i)}{\gamma_\alpha(i)}$$

$$+ \frac{1}{2}\sum_{i=1}^{p}\frac{\tilde{\theta}_k^T(i)\tilde{\theta}_k(i)}{\gamma_k(i)} + \frac{1}{2}\sum_{i=1}^{p}\frac{\tilde{\theta}_\mu^T(i)\tilde{\theta}_\mu(i)}{\gamma_\mu(i)} \qquad (24)$$

where $\tilde{\theta}_\alpha(i) = \theta_\alpha(i) - \theta_\alpha^*(i)$, $\tilde{\theta}_k(i) = \theta_k(i) - \theta_k^*(i)$ and $\tilde{\theta}_\mu(i) = \theta_\mu(i) - \theta_\mu^*(i)$; $\gamma_\alpha(i)$, $\gamma_k(i)$ and $\gamma_\mu(i)$ are positive constants.

Considering Equations (15), (18) and (22), the time derivative of (24) gives

$$\dot{v} = \sum_{i=1}^{p}\dot{v}_i = \sum_{i=1}^{p}\left(s_i(\hat{u}_c(i) - \varphi_i) + \frac{1}{\gamma_\alpha(i)}\dot{\theta}_\alpha^T(i)\tilde{\theta}_\alpha(i)\right.$$

$$\left. + \frac{1}{\gamma_k(i)}\dot{\theta}_k^T(i)\tilde{\theta}_k(i) + \frac{1}{\gamma_\mu(i)}\dot{\theta}_\mu^T(i)\tilde{\theta}_\mu(i)\right) \qquad (25)$$

Let $u_\alpha^*(i) = \xi_\alpha^T(i)\theta_\alpha(i)|s_i| = -\alpha_i^* s_i$, $u_k^*(i) = \xi_k^T(i)\theta_k(i)$ $t_i^r = -k_i^*\int_0^{t_i^r}\text{sign}(s_i)\,dt$ and $u_\mu^*(i) = \xi_\mu^T(i)\theta_\mu(i)|\omega_i(s_i)|$ $= -\mu_i^*\omega_i(s_i)$ denote, respectively, the optimal control laws of $u_\alpha(i)$, $u_k(i)$ and $u_\mu(i)$ that ensure the best tracking control performance of the system (7) by generating the optimal gains α_i^*, k_i^* and μ_i^* of the control law $u_c(i)$, which allows to effectively reject the perturbation φ acting on the system dynamics by verifying the condition (19) while simultaneously ensuring that the undesired chattering are avoided. Then, by introducing the optimal control law $u_c^*(i) = u_\alpha^*(i) + u_k^*(i) + u_\mu^*(i)$

into (25), it gives for $\dot{v}_i$ ($i = 1,\ldots,p$):

$$\dot{v}_i = s_i((\hat{u}_c(i) - u_c^*(i) + u_c^*(i) - \varphi_i) + \frac{1}{\gamma_\alpha(i)}\dot{\theta}_\alpha^T(i)\tilde{\theta}_\alpha(i)$$

$$+ \frac{1}{\gamma_k(i)}\dot{\theta}_k^T(i)\tilde{\theta}_k(i) + \frac{1}{\gamma_\mu(i)}\dot{\theta}_\mu^T(i)\tilde{\theta}_\mu(i)$$

$$= s_i(\xi_\alpha^T(i)\tilde{\theta}_\alpha(i)|s_i| + \xi_k^T(i)\tilde{\theta}_k(i)t_i^r$$

$$+ \xi_\mu^T(i)\tilde{\theta}_\mu(i)|\omega_i(s_i)|) + s_i(u_\alpha^*(i)$$

$$+ u_k^*(i) + u_\mu^*(i) - \varphi_i) + \frac{1}{\gamma_\alpha(i)}\dot{\theta}_\alpha^T(i)\tilde{\theta}_\alpha(i)$$

$$+ \frac{1}{\gamma_k(i)}\dot{\theta}_k^T(i)\tilde{\theta}_k(i) + \frac{1}{\gamma_\mu(i)}\dot{\theta}_\mu^T(i)\tilde{\theta}_\mu(i)$$

$$= \left(s_i^2\text{sign}(s_i)\xi_\alpha^T(i) + \frac{1}{\gamma_\alpha(i)}\dot{\theta}_\alpha^T(i)\right)\tilde{\theta}_\alpha(i)$$

$$+ \left(s_i\xi_k^T(i)t_i^r + \frac{1}{\gamma_k(i)}\dot{\theta}_k^T(i)\right)\tilde{\theta}_k(i)$$

$$+ \left(s_i\xi_\mu^T(i)|\omega_i(s_i)| + \frac{1}{\gamma_\mu(i)}\dot{\theta}_\mu^T(i)\right)\tilde{\theta}_\mu(i)$$

$$+ s_i\left(-\alpha_i^* s_i - k_i^*\int_0^{t_i^r}\text{sign}(s_i)dt - \mu_i^*\omega_i(s_i) - \varphi_i\right)$$

$$(26)$$

Substituting $\dot{\theta}_\alpha(i)$, $\dot{\theta}_k(i)$ and $\dot{\theta}_\mu(i)$ by their expressions defined in (23), gives

$$\dot{v}_i = -|s_i|(\alpha_i^*|s_i| + k_i^* t_i^r + \mu_i^*|\omega_i(s_i)|) - s_i\varphi_i \quad (27)$$

The above equation becomes negative if the following condition is guaranteed:

$$\alpha_i^*|s_i| + k_i^* t_i^r + \mu_i^*|\omega_i(s_i)| \geq \phi_i \qquad (28)$$

the inequality (28) is verified since α_i^*, k_i^* and μ_i^* are the optimal estimation gains of α_i, k_i and μ_i that ensure the condition (19), and therefore, the equation $\dot{v} = \sum_{i=1}^{p}\dot{v}_i$ becomes negative. Thus, the proof 2 is completed. ∎

5. Simulations results

5.1. Robot arm dynamic model

To validate the developed approach of control, consider a two-link robot arm actuated by two DC motors as shown in Figure 2.

Let l_1 and l_2 be arm lengths, m_1 and m_2 the masses at the end of each joint axe, and g the gravity acceleration. Also let $q = [\,q_1\ q_2\,]^T$ be the joint variable vector (angular positions vector).

The robot arm system is described by the following equation [49,50]:

$$M(q)\ddot{q} + C(q,\dot{q})\dot{q} + G(q) = u + d \qquad (29)$$
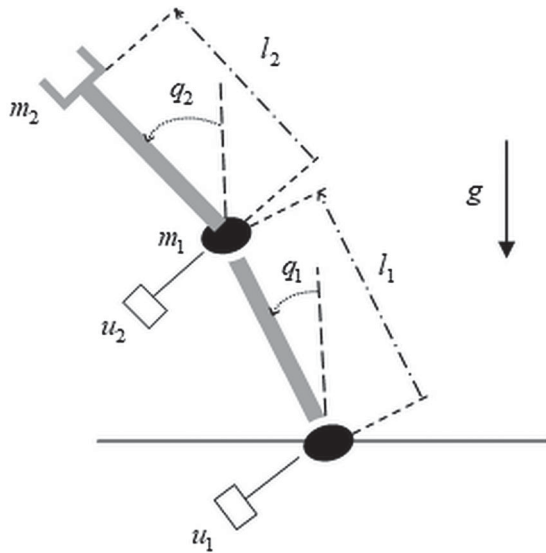
Figure 2. A two-link robot arm.

where $M(q) = \begin{bmatrix} (m_1+m_2)l_1^2 & m_2l_1l_2(\sin(q_1)\sin(q_2) \\ & +(\cos(q_1)\cos(q_2)) \\ m_2l_1l_2(\sin(q_1)\sin(q_2) \\ +(\cos(q_1)\cos(q_2)) & m_2l_2^2 \end{bmatrix}$ is the completed inertia matrix; $C = m_2l_1l_2(\cos(q_1)\sin(q_2) - \sin(q_1)\cos(q_2))\begin{bmatrix} 0 & -\dot{q}_2 \\ -\dot{q}_1 & 0 \end{bmatrix}$ denotes the coriolis and centripetal forces; $G = \begin{bmatrix} -(m_1+m_1)l_1g\sin(q_1) \\ -m_2l_2g\sin(q_2) \end{bmatrix}^T$ Contains the gravity terms; $u = [\, u_1 \ u_2 \,]^T$ is the control torque vector; $d = [\, d_1 \ d_2 \,]^T$ denotes the unknown disturbances, including un-modeled dynamics such as friction force and unknown external disturbances.

Introduce the state vector $\underline{x} = [\, x^T \ \dot{x}^T \,]^T = [\, q^T \ \dot{q}^T \,]^T$, where $x = [\, x_1 \ x_2 \,]^T = [\, q_1 \ q_2 \,]^T$; thus, Equation (29) can be reformulated as

$$\ddot{x} = f_N(\underline{x}) + g_N(x)u + D \tag{30}$$

where $f_N = M^{-1}(-C\dot{q} - G)$, $g_N(x) = M^{-1}$ and $D = M^{-1}d$.

Assume that the mass of joints of the robot arm system (30) presents parametric variation. Therefore,

Equation (30) can be rewritten as

$$\ddot{x} = (f_N(\underline{x}) + \Delta f(\underline{x})) + (g_N(x) + \Delta g(x)u) + \Delta$$
$$= f_N(\underline{x}) + g_N(x)u + \bar{\Delta} \tag{31}$$

where $\Delta f(\underline{x})$ and $\Delta g(x)$ represent the time varying disturbances acting on the system dynamics caused by the mass variation dm; $\Delta = (M + \Delta M)^{-1}d$, with ΔM represents the parametric variation of the inertia matrix M caused by dm; and $\bar{\Delta} = \Delta f(\underline{x}) + \Delta g(x)u + \Delta$.

Equation (31) is similar to the systems described in (7), it is a second-order nonlinear system having two inputs and two outputs, unknown dynamics f_N and g_N, and unknown disturbance vector $\bar{\Delta}$. So, we can apply the proposed control law defined in (22).

5.2. Simulation

A robot arm with the following nominal characteristics is considered:
$l_1 = l_2 = 1$ m; $m_1 = 4$ kg and $m_2 = 2$ kg; $g = 9.8$ m/s^2.

The time varying disturbances on the mass of joins are given as follows: dm (kg) $= [\, dm_1 \ dm_2 \,]^T = [\, 2\sin(t) \ \sin(t) \,]^T$

The unknown disturbances vector is represented as $\bar{\Delta} = (M + \Delta M)^{-1} \begin{bmatrix} 0.8\sin(2t)+0.4\sin(\dot{q}_1)+0.2q_1 \\ 0.6\sin(2t)+0.2\sin(\dot{q}_2)+0.2q_2 \end{bmatrix} + \Delta f(\underline{x}) + \Delta g(x)u$.

Set the initial condition joint angular position vector x (rad) $= [\, 1.2 \ 0.4 \,]^T$.

Set the sliding surfaces $s_1 = \dot{e}_1 + \lambda_1 e_1$ and $s_2 = \dot{e}_2 + \lambda_2 e_2$, where $e_1 = q_{1d} - q_1$ and $e_2 = q_{2d} - q_2$ are the tracking errors, λ_1 and λ_2 are the positive slopes of the sliding surface s_1 and s_2, respectively.

Assume that q_1 and q_2 belong to $[\, -\frac{\pi}{2} \ \frac{\pi}{2} \,]$.

The control objective is to maintain the system to track the desired trajectory $q_d = [\, q_{1d} \ q_{2d} \,]^T = [\, \sin(t) \ \cos(t) \,]^T$.
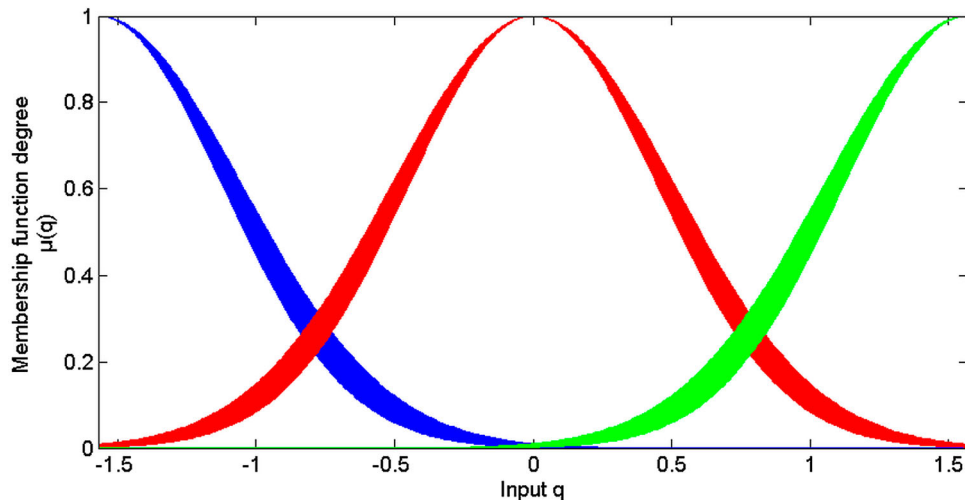
Figure 3. Interval type-2 fuzzy sets used by the IT2-FLS defined in (33).
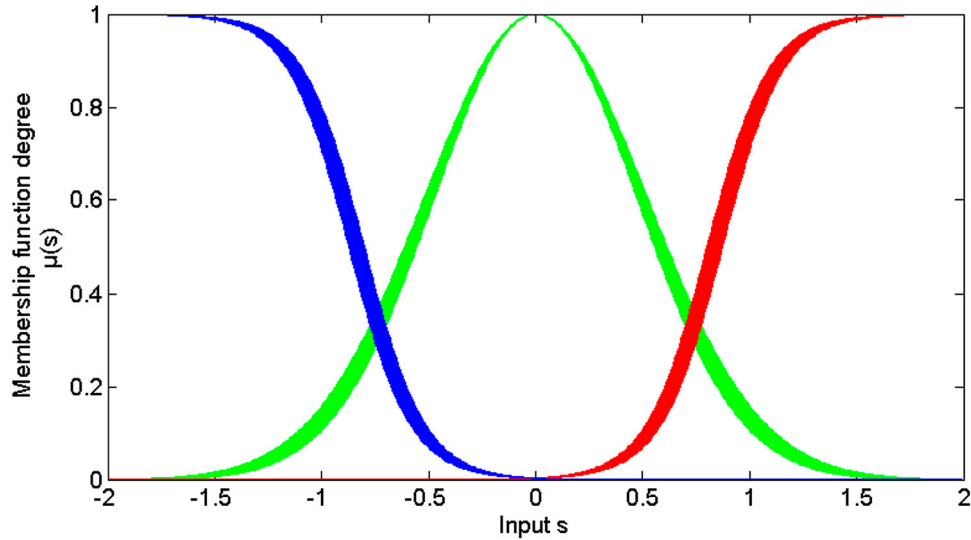
Figure 4. Interval type-2 fuzzy sets used by IT2-FLS $\hat{u}_c$.
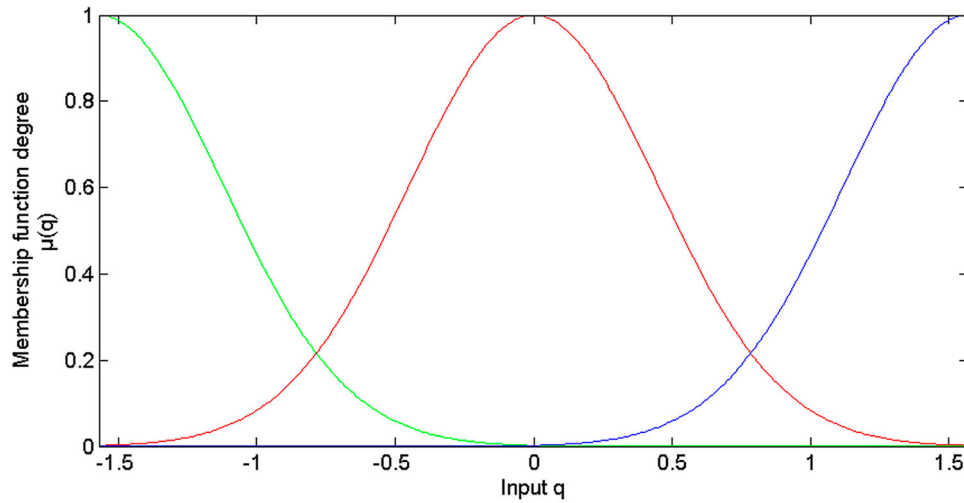
Figure 5. Type-1 fuzzy sets used by the T1-FLS defined in (34).

The proposed AIT2-FSMCL is designed as

$$u = \begin{bmatrix} u_1 & u_2 \end{bmatrix}^{\mathrm{T}}$$
$$= g_0^{-1}(x)(\ddot{q}_d - f_0(\underline{x}) + \rho - \hat{u}_c) \qquad (32)$$

where $\rho = \begin{bmatrix} \lambda_1 & 0 \\ 0 & \lambda_2 \end{bmatrix} \begin{pmatrix} \dot{e}_1 \\ \dot{e}_2 \end{pmatrix}$.

The IT2-FLS used to describe the nonlinear system dynamics (30) is designed as

$$\begin{cases} \dot{x} = f_0(\underline{x}) + g_0(x)u \\ y = x \end{cases} \qquad (33)$$

The IT2-FLS (33) has two inputs q_1 and q_2, and each of them is defined by three MFs, as depicted in Figure 3.

There are $M = 9$ fuzzy rules to describe the unknown dynamics of the system defined in (30), which requires the following A_j and $B_j$matrices ($j = 1, 2, \ldots, 9$):

$$A_1 = \begin{bmatrix} -0.01 & 0.04 & -10.2 & -8.4 \\ 0.02 & 0.01 & -1 & 1 \end{bmatrix}; \quad A_2 = \begin{bmatrix} 12 & -9 & -1 & 0.4 \\ 0 & 17 & 1 & 0 \end{bmatrix};$$
$$A_3 = \begin{bmatrix} 11 & 7 & -1 & 1 \\ 0 & 0 & 1 & -1 \end{bmatrix}; \quad A_4 = \begin{bmatrix} 18 & 0 & 0.03 & 0.34 \\ 1 & 12 & -1 & 0.01 \end{bmatrix};$$
$$A_5 = \begin{bmatrix} 26 & -8 & -0.04 & 0.01 \\ 0 & 7 & 1 & -0.02 \end{bmatrix}; \quad A_6 = \begin{bmatrix} 11 & 0 & 0.02 & 0.48 \\ 0 & 10 & 1 & -0.08 \end{bmatrix};$$

Table 1. The constant parameters of both control approaches.

Parameters	FSOST-SMC	PAC
λ_1	5	5
λ_2	4	4
N_1	–	0.12
N_2	–	0.15
$\gamma_\alpha(1)$	–	20
$\gamma_\alpha(2)$	–	750
$\gamma_k(1)$	–	820
$\gamma_k(2)$	–	1480
$\gamma_\mu(1)$	–	30
$\gamma_\mu(2)$	–	40
b_1	20	–
b_2	38	–
β_1	11	–
β_2	14	–

$$A_7 = \begin{bmatrix} 10 & 4 & -0.04 & 0 \\ 0 & 0.04 & 1 & -1 \end{bmatrix}; \quad A_8 = \begin{bmatrix} 12 & 1 & 0 & -0.4 \\ 0 & 18 & -1 & -0.04 \end{bmatrix}$$
$$A_9 = \begin{bmatrix} 3 & 3 & -1 & 1 \\ 1 & -1 & 0 & 0 \end{bmatrix}; \quad B_1 = \begin{bmatrix} 0.8 & -0.8 \\ -0.8 & 2.4 \end{bmatrix}; \quad B_2 = \begin{bmatrix} 0.54 & 0 \\ 0 & 1.7 \end{bmatrix};$$
$$B_3 = \begin{bmatrix} 0.8 & 0.8 \\ 0.8 & 2.4 \end{bmatrix}; \quad B_4 = B_2; \quad B_5 = B_1; \quad B_6 = B_2; \quad B_7 = B_3$$
$$B_8 = B_2; \quad B_9 = B_1.$$

For the AIT2-FLS $\hat{u}_c$, three MFs are designed for each of its inputs s_1 and s_2, as represented in Figure 4.
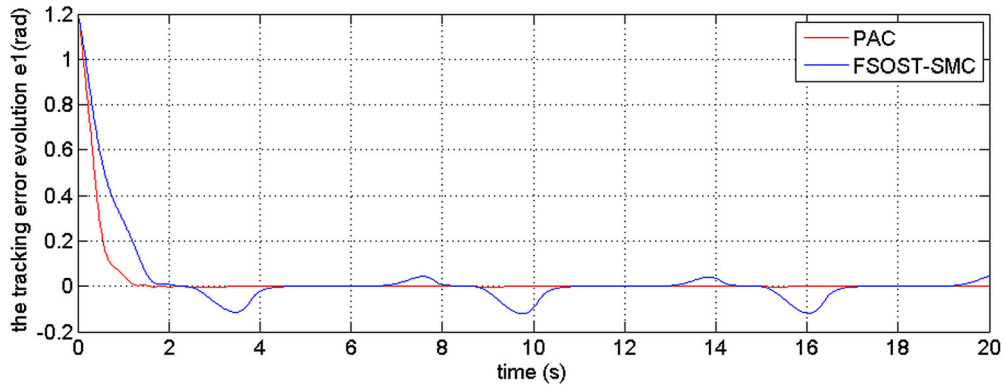
Figure 6. The tracking error e_1(rad) of both control methods.
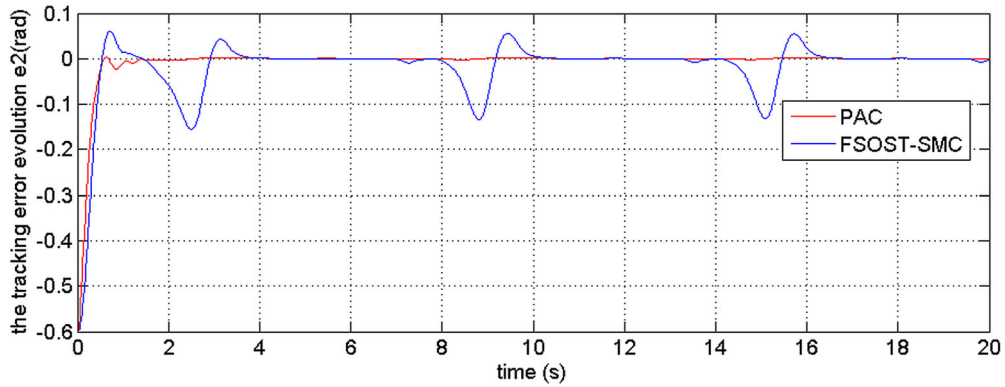
Figure 7. The tracking error e_2(rad) of both control methods.
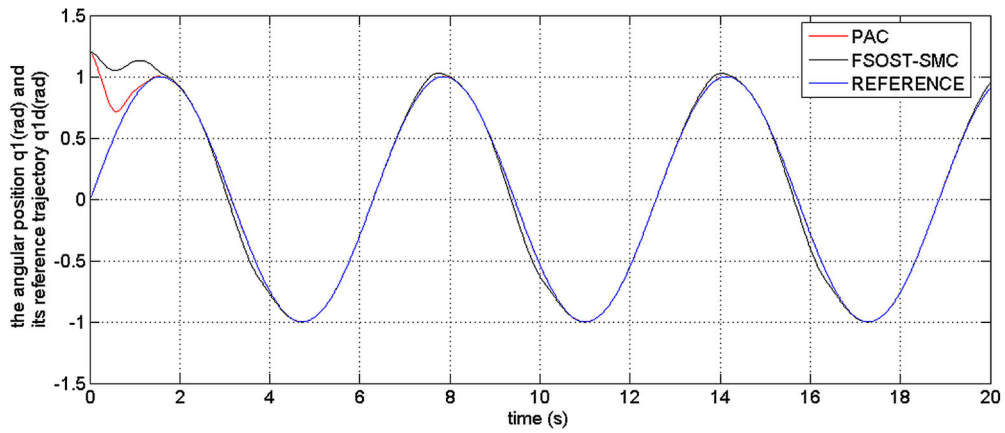
Figure 8. The angular position q_1(rad) and its reference trajectory q_{1d}(rad) of both control methods.
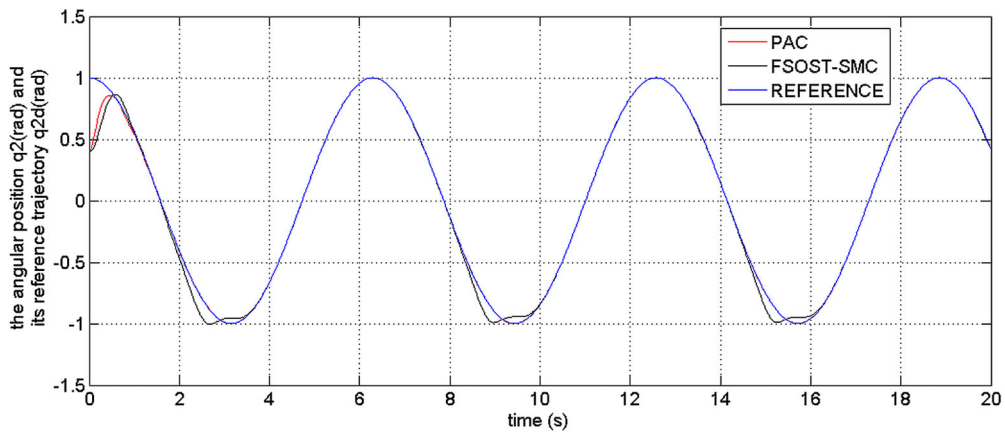
Figure 9. The angular position q_2(rad) and its reference trajectory q_{2d}(rad) of both control methods.
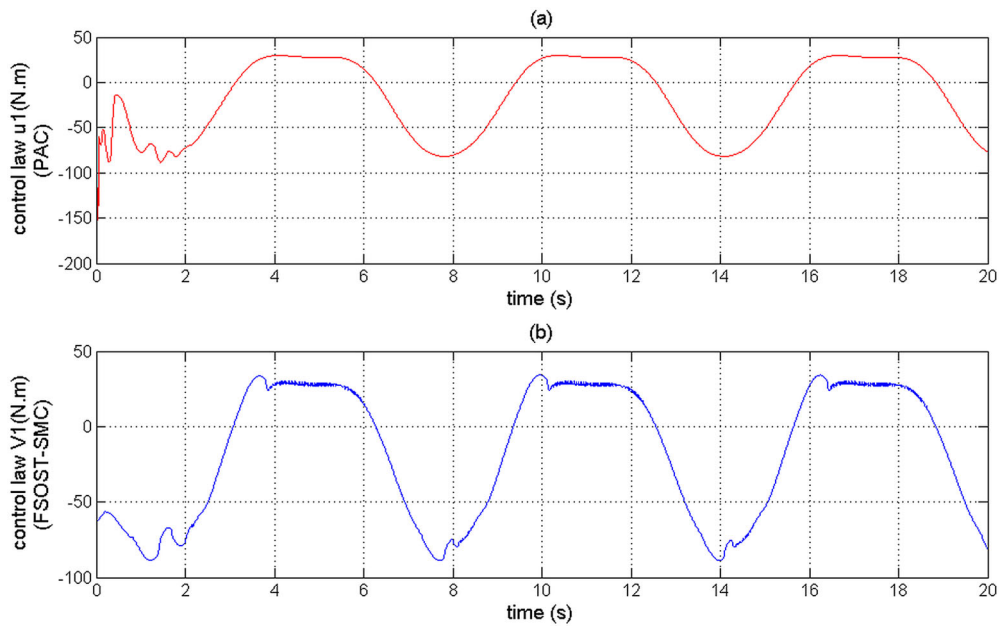
Figure 10. (a) The control law u_1(N.m) of the PAC. (b) The control law V_1(N.m) of the FSOST-SMC approach.
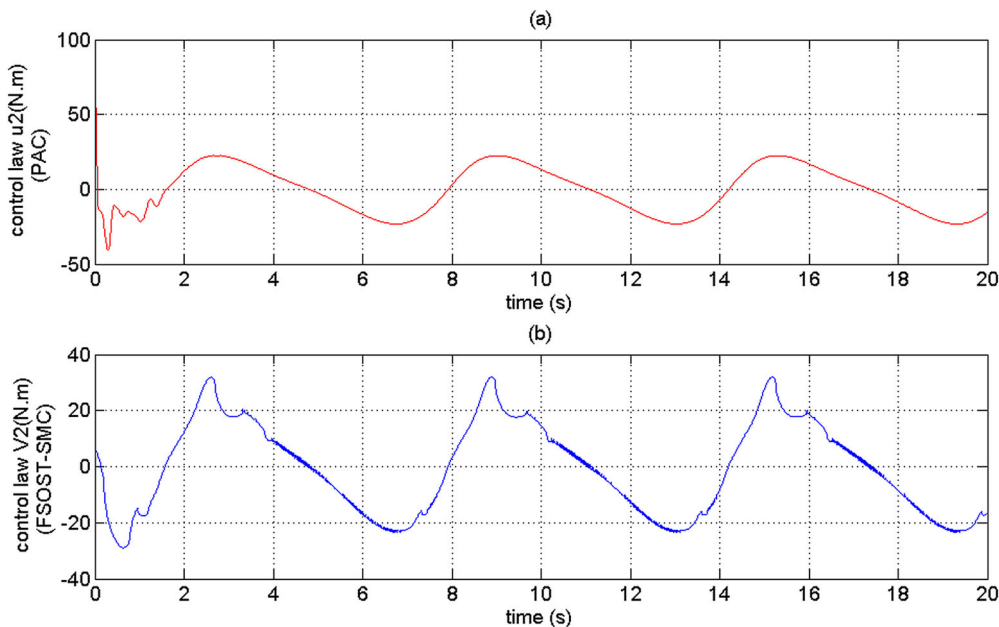
Figure 11. (a) The control law u_2(N.m) of the PAC. (b) The control law V_2(N.m) of the FSOST-SMC approach.
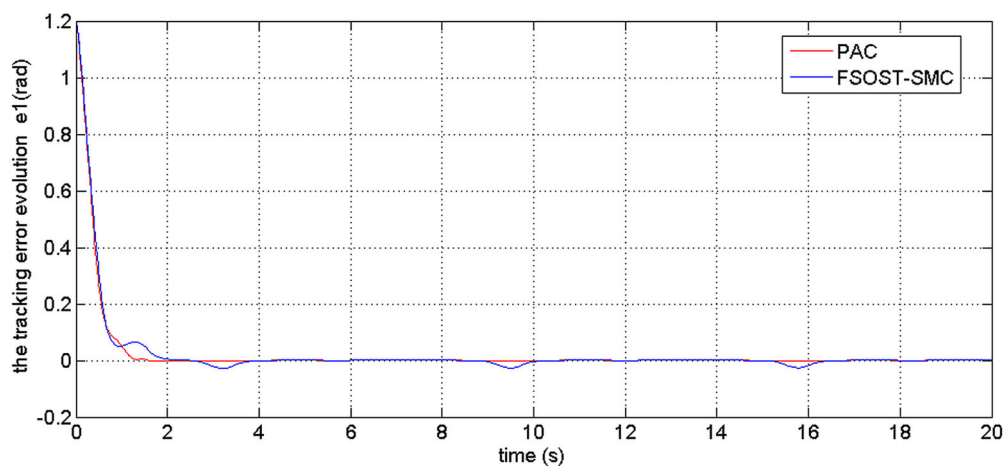
Figure 12. The tracking error e_1(rad) of both control methods, for $b_1 = 27$, $b_2 = 45$, $\beta_1 = 18$ and $\beta_2 = 27$.
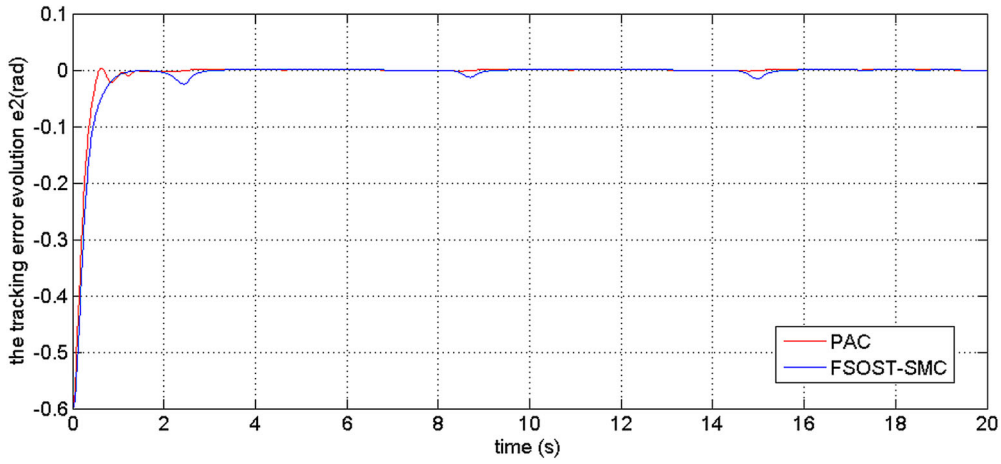
Figure 13. The tracking error e_2(rad) of both control methods, for $b_1 = 27$, $b_2 = 45$, $\beta_1 = 18$ and $\beta_2 = 27$.
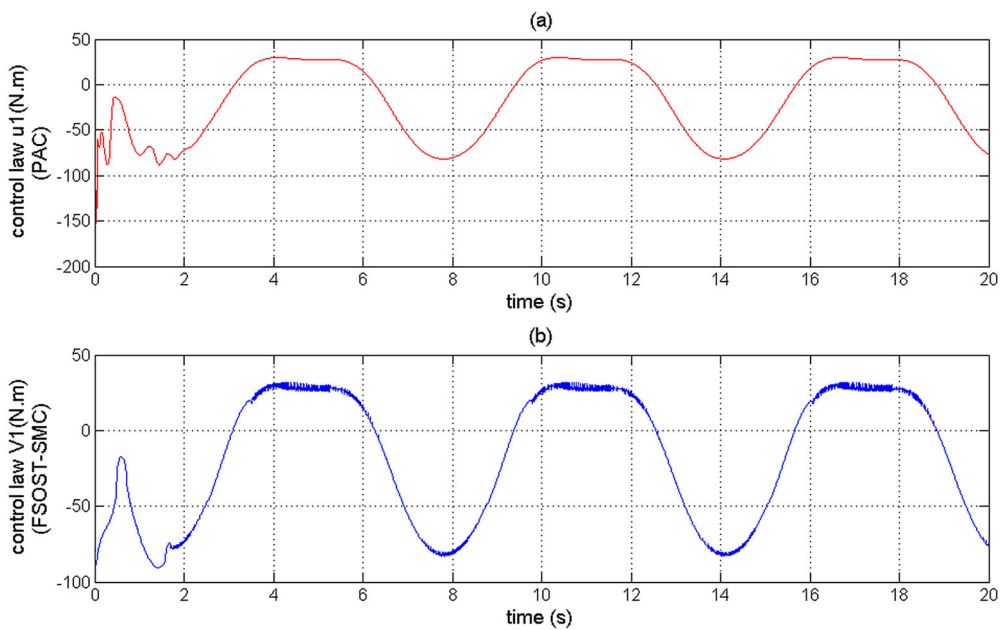
Figure 14. (a) The control law u_1(N.m) of the PAC; (b) The control law V_1(N.m) of the FSOST-SMC approach, for $b_1 = 27$, $b_2 = 45$, $\beta_1 = 18$ and $\beta_2 = 27$.

To show the effectiveness of the proposed approach of control (PAC), a comparison was made with the fuzzy SOST-SMC algorithm (FSOST-SMC) that uses a T1-FLS to approximate the dynamics of the system (30) and uses a SOST-SMC law to handle the approximation errors and unknown disturbances.

The T1-FLS used to describe the nonlinear system dynamics (30) is designed as

$$\begin{cases} \ddot{x} = \bar{f}_0(\underline{x}) + \bar{g}_0(x)V \\ y = x \end{cases} \tag{34}$$

where $\bar{f}_0(\underline{x}) = \sum_{k=1}^{3}\sum_{p=1}^{3}\xi_p^k A_p^k \underline{x}$ and $\bar{g}_0(x) = \sum_{k=1}^{3}\sum_{p=1}^{3}\xi_p^k B_p^k$, such that: $\xi_p^k = \dfrac{\mu_{E^k}(x_1)\mu_{E^p}(x_2)}{\sum_{l=1}^{3}\sum_{m=1}^{3}\mu_{E^l}(x_1)\mu_{E^m}(x_2)}$,

with E^i ($i = 1, \ldots, 3$) are the antecedents T1-FSs characterized by the fuzzy MFs $\mu_{E^i}(x_j)$, $j = 1, 2$, $A_1^1 = A_1$,

$A_2^1 = A_2$, $A_3^1 = A_3$, $A_1^2 = A_4$, $A_2^2 = A_5$, $A_3^2 = A_5$, $A_1^3 = A_7$, $A_2^3 = A_8$, $A_3^3 = A_9$, $B_1^1 = B_1$, $B_2^1 = B_2$, $B_3^1 = B_3$, $B_1^2 = B_4$, $B_2^2 = B_5$, $B_3^2 = B_6$, $B_1^3 = B_7$, $B_2^3 = B_8$, $B_3^3 = B_9$; V denotes the global control law of the FSOST-SMC approach, and is given by the following equation:

$$V = \begin{bmatrix} V_1 & V_2 \end{bmatrix}^{\mathrm{T}}$$
$$= \bar{g}_0^{-1}(x)(\ddot{q}_d - \bar{f}_0(\underline{x}) + \rho - u_{ST}) \tag{35}$$

where $u_{ST} = -\begin{bmatrix} b_1 & 0 \\ 0 & b_2 \end{bmatrix}\begin{bmatrix} \int_0^t \mathrm{sign}(s_1)\mathrm{d}t \\ \int_0^t \mathrm{sign}(s_2)\mathrm{d}t \end{bmatrix} - \begin{bmatrix} \beta_1 & 0 \\ 0 & \beta_2 \end{bmatrix}$
$\begin{bmatrix} |s_1|^{0.5} \\ |s_2|^{0.5} \end{bmatrix}$, with b_1, b_2, β_1 and β_2 are the gains of the SOST-SMC law u_{ST}.

The T1-FSs E^i used by the T1-FLS defined in (34) are depicted in Figure 5.
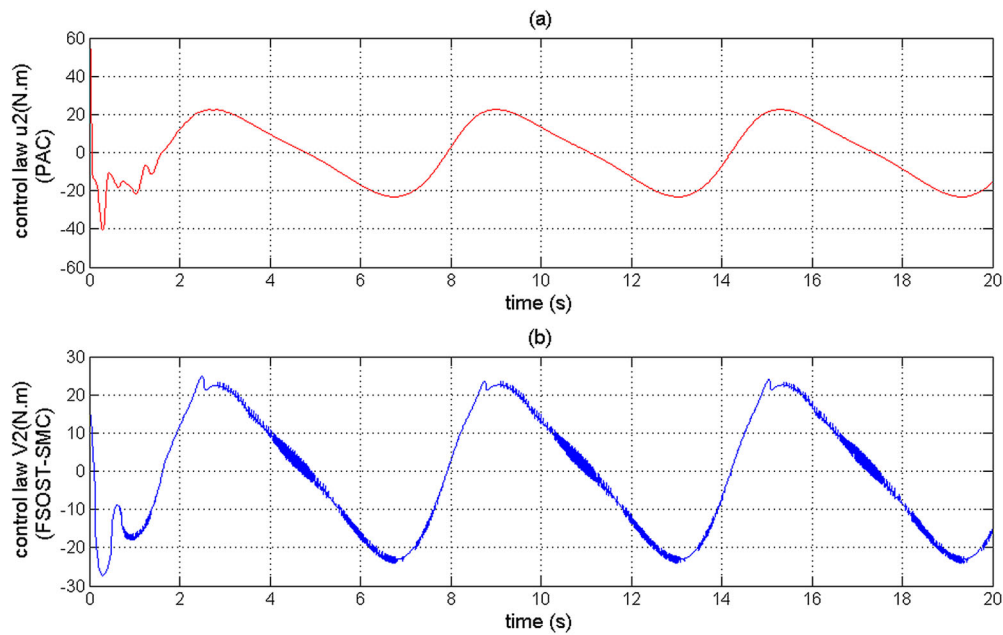
Figure 15. (a) The control law u_2(N.m) of the PAC; (b) The control law V_2(N.m) of the FSOST-SMC approach, for $b_1 = 27$, $b_2 = 45$, $\beta_1 = 18$ and $\beta_2 = 27$.

For the constant parameters of the two approaches of control, we take the following values, as shown in Table 1.

The simulation results are shown in Figures 6–11. They illustrate the comparison between the PAC and the FSOST-SMC method.

Figures 6 and 7, they depict the evolution of the tracking errors. Figures 8 and 9, they represent the trajectories of robot arm angular positions q_1 and q_2, and their references trajectories q_{1d} and q_{2d}, respectively. Figures 10 and 11, they depict the evolution of the control laws of both control methods.

According to the above simulation results, we notice that the PAC ensures the best tracking performance compared to the FSOST-SMC method. This is due to the fact that the PAC, firstly, it efficiently describes the unknown dynamics of the controlled system, and secondly, it rejects the effect of approximation errors, neglected and un-modeled dynamics, time varying disturbances acting on the system dynamics, and unknown external disturbances that perturb the control system more efficiently than the FSOST-SMC approach. Furthermore, the PAC generates smooth control inputs while simultaneously ensuring higher tracking performance. On the other hand, Figures 12–15, they show that when we apply higher gains $(b_1, b_2, \beta_1$ and $\beta_2)$ of the control law u_{ST} of FSOST-SMC in order to improve the tracking performance, the chattering becomes more severe.

Even with the improvement of the tracking performance of the SOST-SMC method, which obtained at the detriment of the smoothness of the applied control inputs, it is noticed that the PAC still presents the best tracking performance with smooth generated control inputs.

6. Conclusion

In this paper, we presented a new robust AIT2-FSMCL for a quite large class of MIMO nonlinear processes with unknown dynamics and subject to unknown disturbances. Firstly, the unknown dynamics have been approximated to a weighted combination of IT2 fuzzy local models. And secondly, a new AIT2-FSMS, which uses three AIT2-FLSs, has been designed to estimate the optimal gains of the AIT2-FSMCL that provide the best tracking performance while simultaneously avoiding the undesired chattering, despite approximation errors and unknown disturbances that affect the studied system, including un-modeled dynamics, parametric variations and unknown external disturbances. The closed-loop system control is globally asymptotically stable and mathematically proven. The simulation example confirms the efficiency of the developed control approach in achieving the desired objectives.

Disclosure statement

No potential conflict of interest was reported by the authors.

ORCID

Mostafa Mjahed http://orcid.org/0000-0001-7661-2095

References

[1] Gao Y, Sh T, Li Y. Observed-based adaptive fuzzy output constrained control for MIMO nonlinear systems with unknown control directions. Fuzzy Sets Syst. 2016;290:79–99.

[2] Liu YJ, Sh T. Adaptive fuzzy identification and control for a class of nonlinear pure-feedback MIMO systems with unknown dead zones. IEEE Trans Fuzzy Syst. 2015;5:1387–1398.

[3] Vijayan A, Ashok S. A MIMO approach to supervisory control in robot visual feedback. Int Rev Model Simul. 2017;10(1):16–25.

[4] Qian D, Sh T, Lee S. Fuzzy-logic-based Control of payload Subjected to Double-Pendulum Motion in Overhead Cranes. Aut Const. 2016;65:133–143.

[5] Moezi SA, Zakeri E, Lari YB, et al. Fuzzy logic control of a ball on sphere system. Adv Fuzzy Syst. 2014;2014:6.

[6] Krokavec D, Filasova A. Stabilizing fuzzy output control for a class of nonlinear systems. Adv Fuzzy Syst. 2013;2013:9.

[7] Londhe PS, Santhakumar M, Patre BM, et al. Task space control of an autonomous underwater vehicle manipulator system by robust single-input fuzzy logic control scheme. IEEE J Ocean Eng. 2017;42(1):13–28.

[8] Chen Z, Zh L, Chen CL. Disturbance observer-based fuzzy control of uncertain MIMO mechanical systems with input nonlinearities and its application to robotic exoskeleton. IEEE Trans Cybern. 2017;47(4):984–994.

[9] Raimondi FM, Melluso M. A new fuzzy robust dynamic controller for autonomous vehicles with nonholonomic constraints. Rob Auton Syst. 2005;52(2–3):115–131.

[10] Wang LX. Stable adaptive fuzzy control of nonlinear systems. IEEE Trans Fuzzy Syst. 1993;1(2):146–155.

[11] Kowalska TO, Dybkowski M, Szabat K. Adaptive sliding-mode neuro-fuzzy control of the two-mass induction motor drive without mechanical sensors. IEEE Trans Ind Elect. 2010; 57(2):553–564.

[12] Sh Y, Shi P, Yang H. Adaptive fuzzy control of strict-feedback nonlinear time-delay systems with unmodeled dynamics. IEEE Trans Cybern. 2016;46(8):1926–1938.

[13] Tayebihaghighi SH, Piltan F, Kim JM. Control of an uncertain robot manipulator using an observation-based modified fuzzy sliding mode controller. Int J Intelligent Syst Appl. 2018;10(3):41–49.

[14] Wen SH, Chen MZQ, Zeng ZH. Adaptive neural-fuzzy sliding-mode fault-tolerant control for uncertain nonlinear systems. IEEE Trans Syst Man Cybernetics: Syst. 2017;47(8):2268–2278.

[15] Yen VTH, Nan WY, Cuong PHV, et al. Robust adaptive sliding mode control for industrial robot manipulator using fuzzy wavelet neural networks. Int J Control Aut Syst. 2017;15(6):2930–2941.

[16] Mao Q, Dou L, Zng Q, et al. Attitude controller design for reusable launch vehicles during reentry phase via compound adaptive fuzzy H-infinity control. Aeorospace Sci Technol. 2018;72:36–48.

[17] Li H, Wang J, Shi P. Output-feedback based sliding mode control for fuzzy systems with actuator saturation. IEEE Trans Fuzzy Syst. 2016;24(6):1282–1293.

[18] Yoshimura T. Design of an adaptive fuzzy sliding mode control for uncertain discrete-time nonlinear systems based on noisy measurements. Int J Syst Sci. 2016;47(3):617–630.

[19] Han H, Lam HK. Discrete sliding-mode control for a class of T-S fuzzy models with modeling error. J Adv Comp Intelligence Intelligent Inform. 2014;18(6):908–917.

[20] Sh I, Liu XP. Robust sliding mode control for robot manipulators. IEEE Trans Ind Elect. 2011;58(6):2444–2453.

[21] Han Y, Kao Y, Gao C. Robust sliding mode control for uncertain discrete singular systems with time-varying delays and external disturbances. Automatica. 2017;75:210–216.

[22] Zhu Q, Yao D, Wang J, et al. Robust control of uncertain semi-Markovian jump systems using sliding mode control method. Appl Math Comp. 2016;286:72–87.

[23] Alonge F, Cirrincione M, D'lppolito F, et al. Robust active disturbance rejection control of induction motor systems based on additional sliding-mode component. IEEE Trans Ind Elect. 2017;64(7):5608–56211.

[24] Qian D, Sh T, Ch L. Leader-following formation control of multiple robots with uncertainties through sliding mode and nonlinear disturbance observer. ETRI J. 2016;38(5):1008–1018.

[25] Utkin V, Lee H. Chattering problem in sliding mode control systems. International workshop on variable structure systems VSS'06, Italy. 2006.

[26] Levant A. Chattering analysis. IEEE Trans Aut Control. 2010;55(6):1380–1389.

[27] Suryawanshi P, Shendge PD, ShB P. A boundary layer sliding mode control design for chatter reduction using uncertainty and disturbance estimator. Int J Dynamics Control. 2016;4(4):456–565.

[28] Goel A, Swarup A. Chattering free trajectory tracking control of a robotic manipulator using high order sliding mode. In: Bhatia SK, Mishra KK, Tiwari S, et al. editors. Advances in computer and computational sciences. Singapore: Springer; 2017. p. 753–761.

[29] Zhang X, Ch Y, Bai H. Fixed-boundary-layer sliding-mode and variable switching frequency control for a bidirectional DC-DC converter in hybrid energy storage system. Electric Power Components Syst. 2017; 45(13):1474–1485.

[30] Zhang Y, Li R, Xue T, et al. An analysis of the stability and chattering reduction of high-order sliding mode tracking control for a hypersonic vehicle. Inf Sci (Ny). 2016;348:25–48.

[31] Rafiq M, Rehman SU, Rehman FU, et al. A second order sliding mode control design of a switched reluctance motor using super twisting algorithm. Simul Model Pract Theory. 2012;25:106–117.

[32] Nagesh I, Edwards CH. A multivariable super-twisting sliding mode approach. Automatica. 2014;50(3):984–988.

[33] Derafa L, Benallegue A, Fridman L. Super-twisting control algorithm for the attitude tracking of a four rotors UAV. J Franklin Inst. 2012;349(2):685–699.

[34] Utin VI, Poznyak AS. Adaptive sliding mode control with application to super-twist algorithm: equivalent control method. Automatica. 2013;49(1):39–47.

[35] Jeong CHS, Kim JSH, Han SL. Tracking error constrained super-twisting sliding mode control for robotic systems. Int J Control, Aut Syst. 2018;116(2):804–814.

[36] Evangelista C, Puleston P, Valenciaga F, et al. Lyapunov-designed super-twisting sliding mode control for wind energy conversion optimization. IEEE Trans Industrial Electronics. 2013;60(2):538–545.

[37] Levant A. Sliding order and sliding accuracy in sliding mode control. Int J Control. 1993;58(6):1247–1263.

[38] Linda O, Manic M. Uncertainty-robust design of interval type-2 fuzzy logic controller for delta parallel robot. IEEE Trans Ind Inform. 2011;7(1):661–670.

[39] Liu Z, Zhang Y, Wang Y. A type-2 fuzzy switching control system for biped robots. IEEE Trans Syst, Man, Cybernetics. Part C (Appl Rev). 2007;37(6):1202–1213.

[40] Khooban MH, Niknam T, Sha-Sadeghi M. A time-varying general type-II fuzzy sliding mode controller for a class of nonlinear power systems. J Intelligent Fuzzy Syst. 2016;30(5):2927–2937.

[41] Ding SH, Huang X, Ban X, et al. Type-2 fuzzy logic control for underactuated truss-like robotic finger with comparison of a type-1 Case. J Intelligent Fuzzy Syst. 2017;33(4):2047–2057.

[42] Castillo O, Amador-Angulo L, Castro J R, et al. A comparative study of type-1 fuzzy logic systems, interval type-2 fuzzy logic systems and generalized type-2 fuzzy logic systems in control problems. Inf Sci. 2016;354:257–274.

[43] Hsu CHH, Juang CHF. Evolutionary robot wall-following control using type-2 fuzzy controller with species-DE-activated continuous ACO. IEEE Trans Fuzzy Syst. 2013;21(1):100–112.

[44] Kouadria AM, Allaoui T, Denai M, et al. Power quality enhancement in off-grid hybrid renewable energy systems using type-2 fuzzy control of shunt active filter. Intelligent Systems and Applications. Studies in Computational Intelligence. Springer, Cham. 2016;650:345–360.

[45] Takagi T, Sugeno M. Fuzzy identification of systems and Its applications to modeling and control. Reading Fuzzy Sets Intelligent Syst. 1993;SMC-15: 387–403.

[46] Mendel JM. Uncertain rule-based fuzzy logic systems: introduction and new direction. Upper Saddle River (NJ): Prentice Hall PTR; 2001.

[47] Wu D, Mendel JM. Enhanced Karnik-Mendel algorithms. IEEE Trans Fuzzy Syst. 2009;17(4):923–934.

[48] Slotine JJ, Sastry SS. Tracking control of non-linear systems using sliding surfaces, with application to robot manipulations. Int J Control. 2007;38:465–492.

[49] El Kari A, Essounbuli N, Hamzaoui A. Commande adaptative floue robuste: application à la commande en poursuite d'un robot [Robust fuzzy adaptive control: application to trackig control of a robot]. Phys Chem News. 2003;10:31–38. French.

[50] Fateh MM. On the voltage-based control of robot manipulators. Int J Control Aut Syst. 2008;6(5): 702–712.